

Cite this: *Chem. Sci.*, 2020, 11, 5909

All publication charges for this article have been paid for by the Royal Society of Chemistry

# The role of porphyrin peripheral substituents in determining the reactivities of ferrous nitrosyl species†

Sk Amanullah and Abhishek Dey \*

Ferrous nitrosyl {FeNO}<sup>7</sup> species is an intermediate common to the catalytic cycles of Cd<sub>1</sub>NiR and CcNiR, two heme-based nitrite reductases (NiR), and its reactivity varies dramatically in these enzymes. The former reduces NO<sub>2</sub><sup>-</sup> to NO in the denitrification pathway while the latter reduces NO<sub>2</sub><sup>-</sup> to NH<sub>4</sub><sup>+</sup> in a dissimilatory nitrite reduction. With very similar electron transfer partners and heme based active sites, the origin of this difference in reactivity has remained unexplained. Differences in the structure of the heme d<sub>1</sub> (Cd<sub>1</sub>NiR), which bears electron-withdrawing groups and has saturated pyrroles, relative to heme c (CcNiR) are often invoked to explain these reactivities. A series of iron porphyrinoids, designed to model the electron-withdrawing peripheral substitution as well as the saturation present in heme d<sub>1</sub> in Cd<sub>1</sub>NiR, and their NO adducts were synthesized and their properties were investigated. The data clearly show that the presence of electron-withdrawing groups (EWGs) and saturated pyrroles together in a synthetic porphyrinoid (FeDEsC) weakens the Fe–NO bond in {FeNO}<sup>7</sup> adducts along with decreasing the bond dissociation free energies (BDFE<sub>NH</sub>) of the {FeHNO}<sup>8</sup> species. The EWG raises the E<sup>o</sup> of the {FeNO}<sup>7/8</sup> process, making the electron transfer (ET) facile, but decreases the pK<sub>a</sub> of {FeNO}<sup>8</sup> species, making protonation (PT) difficult, while saturation has the opposite effect. The weakening of the Fe–NO bonding biases the {FeNO}<sup>7</sup> species of FeDEsC for NO dissociation, as in Cd<sub>1</sub>NiR, which is otherwise set-up for a proton-coupled electron transfer (PCET) to form an {FeHNO}<sup>8</sup> species eventually leading to its further reduction to NH<sub>4</sub><sup>+</sup>.

Received 19th March 2020  
Accepted 7th May 2020

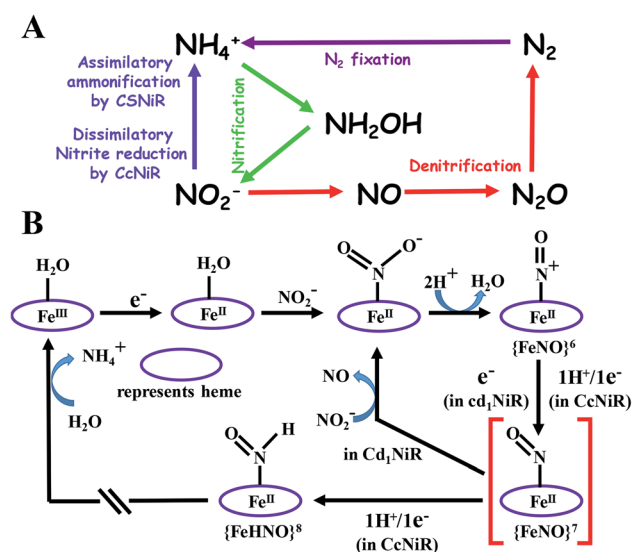
DOI: 10.1039/d0sc01625j

rsc.li/chemical-science

## Introduction

Nitrite plays a vital role in the biochemical N-cycle.<sup>1,2</sup> Being generated from nitrate by the action of a molybdenum-containing nitrate reductase,<sup>3</sup> nitrite is consumed *via* several pathways which involve multiple heme and non-heme enzymes (Scheme 1A).<sup>2</sup> Assimilatory ammonification, catalyzed by siroheme containing nitrite reductase (CSNiR), and dissimilatory nitrite reduction, catalyzed by multi-*c* heme-containing nitrite reductase (CcNiR, Fig. 1A), lead to the formation of ammonium ion (NH<sub>4</sub><sup>+</sup>) directly, without releasing any intermediate nitrogenous species.<sup>4</sup> Alternatively, denitrification involves the reduction of nitrite to nitric oxide (NO), catalyzed by heme *cd*<sub>1</sub> containing nitrite reductase (Cd<sub>1</sub>NiR, Fig. 1B).<sup>5</sup> Further reduction of nitric oxide generates nitrous oxide,<sup>6</sup> which is eventually reduced further to dinitrogen.<sup>7,8</sup> Thus, CcNiR reduces nitrite to NH<sub>4</sub><sup>+</sup> without releasing any intermediate, and Cd<sub>1</sub>NiR reduces

nitrite to release NO. Both of these enzymes have heme cofactors in their active site with a very similar distal environment and electron transfer partners (Fig. 1).



Scheme 1 (A) Selected components of the biochemical cycle of "N" and (B) proposed mechanistic pathways of nitrite reduction catalyzed by CcNiR and Cd<sub>1</sub>NiR.<sup>2</sup>

School of Chemical Sciences, Indian Association for the Cultivation of Science, 2A & 2B Raja SC Mullick Road, Kolkata, India – 700032. E-mail: icad@iacs.res.in

† Electronic supplementary information (ESI) available: Additional NMR, mass, UV-vis and FTIR data, and coordination of the DFT-optimized structures (PDF). CCDC 1854376 (FeDEsP), 1854377 (ZnDEsC) and 1959224 (ZnTEsP). For ESI and crystallographic data in CIF or other electronic format see DOI: 10.1039/d0sc01625j



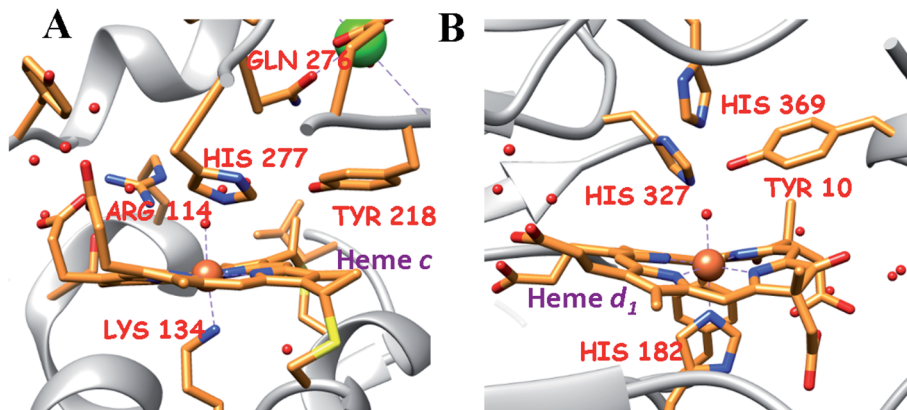


Fig. 1 The active site structure of the nitrite reductases at resting state; (A) CcNiR (pdb: 1FS7)<sup>24</sup> and (B) Cd<sub>1</sub>NiR (pdb: 1NIR);<sup>25</sup> the figures are redrawn using the software package Chimera 1.12rc.

The proposed mechanistic pathways of both Cd<sub>1</sub>NiR and CcNiR are quite similar (Scheme 1B).<sup>2</sup> The nitrite binds to the reduced ferrous iron center. With two protons from the distal residues, a molecule of water is released, forming a {FeNO}<sup>6</sup> intermediate (Enemark–Feltham notation).<sup>5,9,10</sup> The CcNiR avoids the formation of the dead-end intermediate, {FeNO}<sup>7</sup> through two consecutive proton-coupled electron transfer (PCET) to the {FeNO}<sup>6</sup> species, generating an {FeHNO}<sup>8</sup> intermediate,<sup>11</sup> which, on further reduction, leads to the generation of NH<sub>4</sub><sup>+</sup>.<sup>9</sup> Alternatively, Cd<sub>1</sub>NiR forms {FeNO}<sup>7</sup> through an electron transfer (ET) from cytochrome *c*, and releases NO with the concomitant binding of nitrite to the ferrous heme-*d*<sub>1</sub> and the cycle continues.<sup>12–14</sup> The different reactivity of {FeNO}<sup>7</sup> species compels investigating the difference in the active sites that controls the competition between the PCET process and NO release. A {FeNO}<sup>7</sup> adduct generally possesses a very strong Fe–NO bond with a  $K_d \sim 10^{-9}$  and this displacement of NO by nitrite is rather unexpected.<sup>15</sup> Although the N–O stretch of the {FeNO}<sup>7</sup> species of CcNiR is not reported, the N–O stretch of Cd<sub>1</sub>NiR is higher than that of other known heme proteins like hemoglobin and myoglobin.<sup>16–18</sup> We find a strong positive

correlation between the reported rate of NO dissociation and the corresponding N–O frequency (Fig. 2A). It suggests that the rate of NO dissociation is reflected by the strength of the Fe–NO bond, which is reflected in the N–O stretching vibration.<sup>16–21</sup> Similar correlation is also present between the N–O stretching frequency and the rate of NO displacement by pyridine in different synthetic meso-phenyl substituted Fe-porphyrins (Fig. 2B).<sup>22</sup> Iron-porphyrins bearing electron-withdrawing groups (EWGs), having higher N–O stretching frequency, release NO easier. Previous work from our group demonstrated that the iron-porphyrins bearing EWGs and/or saturated  $\beta$ -pyrrolic carbons form weaker iron-nitrosyls due to the competitive back-bonding between macrocycle  $\pi^*$  and NO  $\pi^*$ -orbitals from the filled Fe- $d_{\pi}$  orbitals.<sup>23</sup>

CcNiR and Cd<sub>1</sub>NiR possess basic 2<sup>nd</sup> sphere distal residues and primarily  $\sigma$ -donor histidine or lysine axial ligands and the same redox partner (cytochrome *c*). These residues assist in NO<sub>2</sub><sup>-</sup> binding, proton translocation and are likely to affect the dissociation constants of NO<sub>x</sub> ligands.<sup>9,11,26,27</sup> Another major distinction is the difference in the nitrite binding sites: heme *c* in CcNiR, and heme *d*<sub>1</sub> in Cd<sub>1</sub>NiR (Fig. 1).<sup>24,25</sup> The major



Fig. 2 Correlation between N–O stretching frequency<sup>16–18</sup> and rate of NO dissociation:<sup>19–21</sup> (A) in six-coordinate heme nitrosyls in enzyme systems; (B) in synthetic Fe-porphyrin nitrosyl complexes, TTP (*p*-tolyl), TDFPP (2,6-difluorophenyl), TDCPP (2,6-dichlorophenyl), TPFPP (pentafluorophenyl).





Fig. 3 Structure of the naturally occurring heme and synthetic Fe-porphyrinoids. FeOEP, FeOEPone, and Fe(2,4-OEPdione) were synthesized previously.<sup>32,47,48</sup>

difference in heme  $d_1$ , relative to heme  $c$  is the presence of two saturated  $\beta$ -pyrroles (*i.e.*,  $sp^3$  hybridized peripheral carbons) along with two electron-withdrawing keto-groups (Fig. 3).<sup>28,29</sup> Therefore, their divergent reactivity may stem from differences in the structure of iron-porphyrinoid macrocycles. To evaluate this possibility, the electrochemistry of synthetic iron-porphyrin model complexes (FeTPP, FeOEP, FeOEPone and Fe(2,4-OEPdione), Fig. 3) and their nitrosyl adducts has been investigated by several groups.<sup>30–39</sup> Under coulometric conditions, nitrite could be reduced to ammonium ion by the synthetic complexes mediated by a hydroxylamine bound species.<sup>40–43</sup> The rate of the reaction was strongly directed by the macrocycle *i.e.*, FeOEP reacted faster than FeTPP and the reaction was very slow in the Fe(2,4-OEPdione) complex. The basicity of  $\{\text{FeNO}\}^8$  species could potentially explain the difference in reactivity.<sup>42</sup> Alternatively, the greater Lewis acidity of  $\{\text{Fe(2,4-OEPdione)-NO}\}^7$  (as suggested by the facile pyridine binding to the

Fe) was suggested to enhance the His-coordination with heme  $d_1$  which might help the release of the *trans* NO.<sup>33</sup> These results herald the intrinsic nature of the macrocycle as a determinant of the different reactivity of the  $\{\text{FeNO}\}^7$  species, *i.e.*, NO release *vs.* PCET. An  $\{\text{FeHNO}\}^8$  species (converted after PCET to  $\{\text{FeNO}\}^7$ ) is quite reactive and so far could only be transiently observed in protected environments such as proteins,<sup>44,45</sup> or in bis-picket fence porphyrin<sup>46</sup> or in highly electron-rich FeOEP in the presence of weak acids such as substituted phenols.<sup>41</sup> Alternatively, under electrochemical conditions,  $\{\text{FeNO}\}^8$  yields the parent  $\{\text{FeNO}\}^7$  species and  $\text{H}_2$ .<sup>43</sup> It is important to understand the role of these peripheral modifications in the electronic structure and reactivity of these iron nitrosyls, to understand the different reactivities of the  $\{\text{FeNO}\}^7$  species exhibited by these enzymes.

In this manuscript, a series of synthetic iron-porphyrins were developed for systematically varying their peripheral





Scheme 2 Synthetic strategy of FeTEsP. In some cases, the  $-\text{CO}_2\text{Et}$  group is abbreviated as "E" for clarity in representation.

substituents. By introducing EWGs and/or saturation at the  $\beta$ -pyrrolic positions, we were able to decode the role of each substituent on the basic iron-porphyrin skeleton in the electronic structure and reactivity of their corresponding  $\{\text{FeNO}\}^7$  species. The electrochemical and spectroscopic data of their NO adducts and density functional theory (DFT) calculations help delineate the contribution of reduction potential and  $\text{p}K_{\text{a}}$  to the bond dissociation free energy ( $\text{BDFE}_{\text{NH}}$ ) of the N–H bond in the  $\{\text{FeHNO}\}^8$  species. The results indicate a definitive role of EWG and saturation in tuning the Fe–NO bond strength, the reduction potential of  $\{\text{FeNO}\}^7$  and  $\text{p}K_{\text{a}}$  of  $\{\text{FeNO}\}^8$  species, which can likely explain the origin of differences in the reactivity of  $\text{CcNiR}$  and  $\text{Cd}_1\text{NiR}$ .

## Results

### Synthesis

The heme involved in the nitrite binding sites of  $\text{CcNiR}$  and  $\text{Cd}_1\text{NiR}$  is heme *c* and heme *d<sub>1</sub>*, respectively. The major

difference between these is the presence of two electron-withdrawing-keto groups and two saturated  $\beta$ -pyrrolic carbons in heme *d<sub>1</sub>* (Fig. 3). To rationalize the effect of the EWG and/or saturation, a series of iron-porphyrinoids were synthesized (Fig. 3), namely, iron-tetraphenylporphyrin (FeTPP, fully unsaturated); iron-diesterporphyrin (FeDEsP, having two electron-withdrawing ester groups); iron-tetraesterporphyrin (FeTEsP, having four ester groups); iron-tetraphenylchlorin (FeTPC, having two saturated  $\beta$ -pyrrolic carbons) and iron-diesterchlorin (FeDEsC, having two ester groups and two saturated  $\beta$ -pyrrolic carbons). The EWGs were designed to qualitatively emulate the  $-\text{I}$  (inductive) effect of the keto-groups in heme *d<sub>1</sub>*. FeTPP, FeTPC, FeDEsP, and FeDEsC complexes were synthesized following previously reported procedures.<sup>23,49</sup>

FeTEsP was synthesized to introduce four electron-withdrawing substitutions on the porphyrin ring. TEsP (5 in Scheme 2) was synthesized by the propionic acid condensation of two dipyrromethanes (Scheme 2), one of which (TESbpyr-dial, 3 in Scheme 2) contained four ester groups (at the 3 and 4



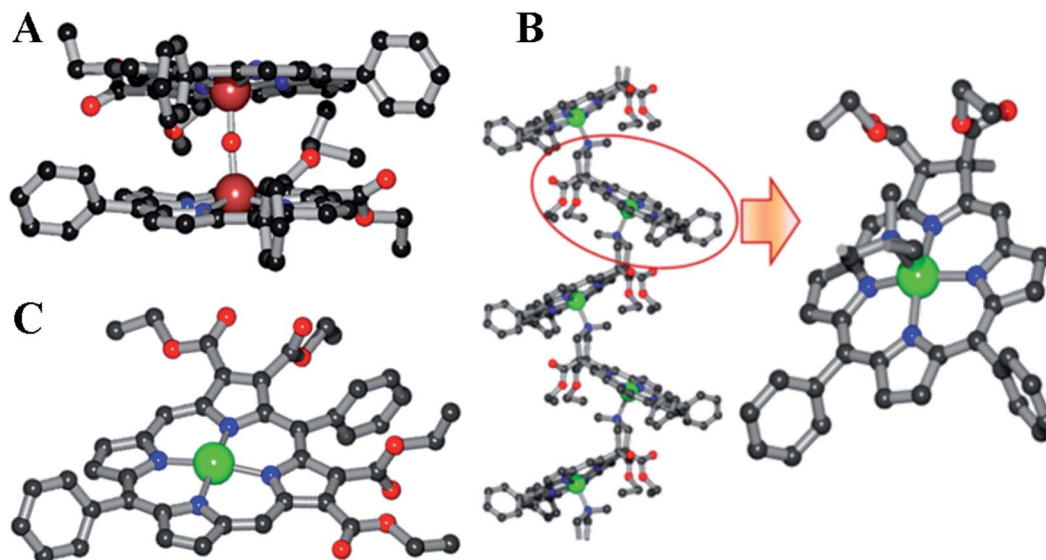


Fig. 4 Molecular structures of the crystals of (A) a  $\mu$ -oxo dimer of FeDEsP; (B) ZnDEsC, and (C) ZnTEsP. Color code: C, black; Fe, brownish-red; Zn, green; N, blue; O, red. Hydrogen atoms are omitted for clarity.

positions of the respective pyrroles) as well as two aldehyde groups (at the 2 positions of the respective pyrroles) and the other half was 5-phenyldipyrromethane (4 in Scheme 2). Base induced cyclization of diethyl fumarate and *p*-toluenesulfonylmethylisocyanide (TosMIC) leads to the formation of a pyrrole bearing two ester groups (DEsPyr, 1 in Scheme 2). The dipyrromethane of DEsPyr (TEsPyr, 2 in Scheme 2) was obtained by the condensation with benzaldehyde under harsh acidic conditions. A Vilsmeier–Haack reaction was performed upon TEsPyr to obtain the corresponding dialdehyde, TEsPyr-dial (3 in Scheme 2).

The other half, *i.e.*, the 5-phenyldipyrromethane (4 in Scheme 2), was prepared by the acid-catalyzed condensation of pyrrole and benzaldehyde following the Lindsey protocol.<sup>50</sup> Zinc and iron metalation was performed using established protocols.<sup>49</sup> The zinc complex of TEsP was characterized by single-crystal XRD. Needle-shaped purple crystals of ZnTEsP were grown from the diffusion of hexane into a chloroform solution of the complex (Fig. 4C). It crystallized in a triclinic symmetry with a centrosymmetric  $P\bar{1}$  space group. Structural analysis revealed that it was a dimer, formed by the coordination of a free carbonyl “oxygen” atom with the zinc atom of another molecule. The structures of FeDEsP and ZnDEsC were reported before and are shown here for comparison (Fig. 4A and B). Further investigations were performed with the nitrosyl adducts of the iron-bound porphyrinoids.

### Iron-nitrosyl reduction potentials

The cyclic voltammograms of the nitrosyl complexes of FeTPP, FeDEsP, FeTEsP, FeTPC, and FeDEsC showed an oxidation process at 0.20, 0.34, 0.38,  $-0.04$  and  $0.10$  V, respectively, against the  $\text{Fc}^+/\text{Fc}$  redox couple (Fig. 5). For FeTPC and FeDEsC, the process was clearly observed only under fast scan rates (Fig. S23B†). The process was irreversible at slow scan rates, indicating dissociation of the NO during oxidation. Note that

the CV of FeDEsC was performed under NO saturation condition to prevent NO loss from the complex. Past research from the Ryan and Kadish group established the nature of these redox events: the oxidation wave of porphyrin  $\{\text{FeNO}\}^7$  leads to the formation of  $\text{Fe}^{\text{III}}\text{-NO}$  species, while in the case of chlorins, bacterio/iso-bacteriochlorins, and porphyrinone/porphinediones, the oxidation leads to the formation of  $\text{Fe}^{\text{II}}\text{-NO}$  species with the macrocycle-cation radical.<sup>32,33,36,51</sup> The  $\{\text{FeNO}\}^{7/8}$  process was observed for FeTPP, FeDEsP, FeTEsP, FeTPC, and FeDEsC at  $-1.41$ ,  $-1.24$ ,  $-1.14$ ,  $-1.51$  and  $-1.42$  V, respectively, vs. the  $\text{Fc}^+/\text{Fc}$  redox couple (Fig. 5). The values obtained for FeTPP were consistent with previous reports.<sup>38</sup> The pre-wave observed in the



Fig. 5 Cyclic voltammograms of the complexes in dichloromethane at room temperature. Working electrode: glassy carbon; counter electrode: platinum; reference electrode: aqueous  $\text{Ag}/\text{AgCl}$  in 4 M KCl; supporting electrolyte: tetrabutylammonium hexafluorophosphate (100 mM); scan rate: 50 mV ps.



case of FeTPP ( $-1.32$  V), FeDEsP ( $-1.17$  V) and FeTPC ( $-1.38$  V) might be due to ligand association, which disappeared at higher scan rates (Fig. S23A†) as reported by the Kadish group earlier.<sup>38,52</sup> In the case of FeDEsC, the irreversible pre-wave at  $\sim -1.22$  V vs. the  $\text{Fe}^+/\text{Fe}$  redox couple was likely due to the direct electrochemical NO reduction<sup>53</sup> (NO saturated solution), as observed by the Kadish group during the reduction of  $\text{Fe}^{\text{II}}\text{-TPP-NO}$  and  $\text{Fe}^{\text{II}}\text{-OEP-NO}$ , in the presence of excess NO gas in the medium.<sup>38</sup>

A clear trend was observed in both the oxidation and reduction process of the  $\{\text{FeNO}\}^7$  species for the series of iron porphyrinoids used here. With an increase in the number of EWGs attached to the  $\beta$ -pyrroles relative to FeTPP-NO, both  $\{\text{FeNO}\}^{6/7}$  and  $\{\text{FeNO}\}^{7/8}$  couples shifted to higher potential (*i.e.*, for FeDEsP-NO and FeTESP-NO in Fig. 5). Alternatively, saturating one of the pyrroles of FeTPP-NO, *i.e.*, in the case of FeTPC-NO, both the reduction couples shifted to lower potentials. The FeDEsC-NO complex, having both EWGs as well as saturated pyrrole centers, had both the reduction potentials

almost similar to those of FeTPP-NO. This implied that the EWG and saturation had opposite effects on the electronic structure of the Fe-NO unit.

### Fe-NO bond strength

The FTIR data of the five-coordinate  $\{\text{FeNO}\}^7$  complexes of FeTPP, FeDEsP, FeTESP, FeTPC, and FeDEsC showed the N-O stretch at  $1676$ ,  $1686$ ,  $1688$ ,  $1680$  and  $1691$   $\text{cm}^{-1}$ , respectively (Fig. 6). The data showed that when two EWGs were introduced (FeDEsP), the N-O vibration (str.) shifted to  $1686$   $\text{cm}^{-1}$  from  $1676$   $\text{cm}^{-1}$  in FeTPP. Further addition of EWGs (FeTESP), shifted the N-O vibration (str.) up to  $1688$   $\text{cm}^{-1}$ . Such high N-O stretching frequencies had only been reported for  $\{\text{FeNO}\}^7$  species of octa-halogenated porphyrins and reflect poor back-bonding between the occupied iron and unoccupied NO  $\pi^*$ -orbitals.<sup>22,54</sup> The saturation of the pyrrole, by itself, exerted little effect on Fe-NO bonding as indicated by the N-O stretching frequency of  $\{\text{FeTPC-NO}\}^7$  at  $1680$   $\text{cm}^{-1}$  which was very similar to that of  $\{\text{FeTPP-NO}\}^7$ . But saturation along with EWGs caused



Fig. 6 FTIR data of the  $\{\text{FeNO}\}^7$  adducts in dichloromethane at room temperature.



a substantial weakening of the NO adduct, as indicated by the N–O stretch of {FeDesC–NO}<sup>7</sup> at 1691 cm<sup>-1</sup>, relative to {FeTPP–NO}<sup>7</sup> at 1676 cm<sup>-1</sup>. The Fe–N stretch of the {FeNO}<sup>7</sup> species of FeTPP–NO reproduced the previously reported value. However, despite several attempts with resonance Raman the Fe–N stretching frequencies could not be obtained for the other compounds studied (Fig. S24A†).<sup>43</sup> The strength of the Fe–NO bond in the {FeNO}<sup>7</sup> adducts was strongly dictated by both  $\sigma$ -bonding and  $\pi$ -back-bonding.<sup>55–58</sup> As reported recently, the presence of electron-withdrawing substitutions on the porphyrin lowers the energy of the porphyrin  $\pi^*$ -orbitals. This results in competitive back-bonding from the filled  $d_{\pi}$  orbitals of Fe between porphyrin  $\pi^*$  and NO  $\pi^*$ -orbitals, which eventually weakens the NO adducts.<sup>23</sup> Saturation by itself had a minor effect on the back-bonding. However, saturation along with two EWGs had an enhanced effect on the weakening of the NO-adduct.

Qualitatively, a similar trend was observed for N-methylimidazole bound six-coordinate {FeNO}<sup>7</sup> species where the N–O stretching vibrations for FeTPP, FeDesP, FeTEsP, FeTPC, and FeDesC were observed at 1626 cm<sup>-1</sup>, 1641 cm<sup>-1</sup>, 1646 cm<sup>-1</sup>, 1635 cm<sup>-1</sup> and 1633 cm<sup>-1</sup>, respectively (Fig. S25A†). Therefore, an axial, primarily  $\sigma$  donor, nitrogenous ligand has a very limited effect on the electronic structure of these {FeNO}<sup>7</sup> complexes. Note that the N–O stretching of the {FeNO}<sup>7</sup> species in Cd<sub>1</sub>NiR was 1626 cm<sup>-1</sup> with heme *d*<sub>1</sub>, relative to 1612 cm<sup>-1</sup> in myoglobin with heme *b* (which neither has an EWG nor saturation).<sup>16–18</sup> The higher N–O stretching frequency in Cd<sub>1</sub>NiR (by 14 cm<sup>-1</sup>) was indicative of a weaker Fe–NO bonding. And it was associated with a  $\sim 10^6$  fold enhancement in NO dissociation rate from the {FeNO}<sup>7</sup> intermediate (Fig. 2).<sup>13,19–21,59</sup> The 15 cm<sup>-1</sup> upshifting of the N–O vibration observed here between FeDesC and FeTPP mirrored the 14 cm<sup>-1</sup> shift observed between Cd<sub>1</sub>NiR and myoglobin suggesting a weakening of the Fe–NO bond, raising the possibility of ligands like NO<sub>2</sub><sup>-</sup> displacing the bound NO.

The displacement of the bound NO from the N-methylimidazole bound six-coordinated {FeNO}<sup>7</sup> species by NO<sub>2</sub><sup>-</sup> was investigated using absorption spectroscopy (see the ESI, Section 8†). The *K*<sub>d</sub> for the process (Fe<sup>II</sup>–NO + NO<sub>2</sub><sup>-</sup>  $\rightleftharpoons$  Fe<sup>II</sup>–NO<sub>2</sub><sup>-</sup> + NO) was determined to be 0.09 for FeTPP and 0.46 for FeDesC (Table 1). The higher *K*<sub>d</sub> for FeDesC, relative to FeTPP, translated to a  $\Delta G$  difference of  $\sim 1$  kcal mol<sup>-1</sup> and correlated very well with its stronger N–O stretching frequency and demonstrated clearly

how the EWG and saturation of the porphyrin ring aid the displacement of NO by NO<sub>2</sub><sup>-</sup>, as proposed for Cd<sub>1</sub>NiR. A similar effect was observed on the displacement rate of NO by pyridine in {FeNO}<sup>7</sup> complexes in a series of iron porphyrins, where the octa-halogenated derivative of TPP was  $\sim 10^6$  times faster than that of FeTPP.<sup>22</sup>

Spectroelectrochemistry was used to access the N–O vibrations of the {FeNO}<sup>6</sup> and {FeNO}<sup>8</sup> species (Table 1, Fig. S26–S28†). The N–O vibrations for the six-coordinate {FeNO}<sup>6</sup> for FeTPP, FeDesP, and FeTEsP were obtained at 1914 cm<sup>-1</sup>, 1923 cm<sup>-1</sup>, and 1927 cm<sup>-1</sup>, respectively (Fig. S27†). The higher N–O vibration for the porphyrins containing EWGs relative to FeTPP mirrored the trend observed for the corresponding {FeNO}<sup>7</sup> species. The N–O vibrations for both five and six-coordinate {FeNO}<sup>6</sup> species of FeTPC and FeDesC could not be obtained, which was consistent with the irreversible CV observed for these species indicating that the {FeNO}<sup>6</sup> species dissociate within the time scale of the experiment (Fig. S23B and S27†). The inability to identify five-coordinate {FeNO}<sup>6</sup> species of FeDesP and FeTEsP again suggested the formation of a labile {FeNO}<sup>6</sup> adduct. The N–O vibrations for the {FeNO}<sup>8</sup> species could be observed for FeTEsP and FeDesC at 1550 cm<sup>-1</sup> and 1537 cm<sup>-1</sup>, respectively (Fig. S28 and Table S2†). The values obtained were consistent with the previously reported values for the five-coordinate {FeNO}<sup>8</sup> porphyrins.<sup>54,60,61</sup> Note that the frequencies were much higher than the value reported for FeTPP at 1496 cm<sup>-1</sup>.<sup>43</sup> Here, too, the inclusion of the EWG and saturation together leads to a substantial increase in the N–O vibration indicating a weakening of the Fe–NO bonding. Thus, the FTIR data for the {FeNO}<sup>6</sup>, {FeNO}<sup>7</sup>, and {FeNO}<sup>8</sup> species all showed that the inclusion of EWG and saturation at the periphery of the porphyrin macrocycle substantially weakened the Fe–NO bonding.

A plot of the experimentally observed N–O vibrations (Table 1) with ln(*K*<sub>d</sub>) for the series of complexes investigated here showed a reasonably linear correlation (Fig. 7) in line with the linear correlation observed between  $\nu$ (N–O) and ln(*k*<sub>off</sub>) (Fig. 2). Thus, the electronic structure responsible for the correlation in the enzyme active site was captured in the series of porphyrins used here – primarily the competitive back-bonding between porphyrin  $\pi^*$  and NO  $\pi^*$ -orbitals adding credence to the use of the electron-withdrawing

Table 1 Properties of {FeNO}<sup>6/7/8</sup> species for the synthetic porphyrins

	{FeNO} <sup>6</sup>	$\rightleftharpoons$	{FeNO} <sup>7</sup>	$\rightleftharpoons$	{FeNO} <sup>8</sup>	
	$\nu_{\text{N-O}}^a$ 5C (6C)	<i>E</i> <sup>c,b</sup>	$\nu_{\text{N-O}}$ 5C (6C)	<i>E</i> <sup>c</sup>	$\nu_{\text{N-O}}$ 5C (6C)	<i>K</i> <sub>d</sub> <sup>e</sup>
FeTPP–NO	1844 (1914)	0.20	1676 (1626)	-1.41	1496 (ref. 43)	0.09 $\pm$ 0.05
FeDesP–NO	<sup>c</sup> (1923)	0.34	1686 (1641)	-1.24	<sup>c</sup>	0.20 $\pm$ 0.04
FeTEsP–NO	<sup>c</sup> (1927)	0.38	1688 (1646)	-1.14	1550	0.23 $\pm$ 0.02
FeTPC–NO	<sup>a</sup>	-0.04 <sup>d</sup>	1680 (1635)	-1.51	<sup>c</sup>	0.13 $\pm$ 0.04
FeDesC–NO	<sup>a</sup>	0.10 <sup>d</sup>	1691 (1633)	-1.42	1537	0.46 $\pm$ 0.04

<sup>a</sup> Stretching frequency in cm<sup>-1</sup>. <sup>b</sup> Potentials are reported vs. Fe<sup>+/0</sup> in dichloromethane. <sup>c</sup> Not observed. <sup>d</sup> Irreversible cathodic waves. <sup>e</sup> Fe<sup>II</sup>–NO + NO<sub>2</sub><sup>-</sup>  $\rightleftharpoons$  Fe<sup>II</sup>–NO<sub>2</sub><sup>-</sup> + NO.







Fig. 8 Formation of  $\text{N}_2\text{O}$  during the electrolysis of  $\{\text{FeDEsP-NO}\}_7$  at  $-1.31$  V (vs.  $\text{Fc}^+/\text{Fc}$ ). On applying potential,  $\text{N}_2\text{O}$  is generated ( $\nu_{\text{N-O}}(14/15)$ :  $2224/2154$   $\text{cm}^{-1}$ ), with the expense of  $\{\text{FeDEsP-NO}\}_7$  peaks ( $\nu_{\text{N-O}}(14/15)$ :  $1684/1657$   $\text{cm}^{-1}$ ): (A) in the presence of  $^{14}\text{NO}$  and (B) in the presence of  $^{15}\text{NO}$ .

the ferric state or the ferrous state of the NO adduct.<sup>1,68</sup> Recent data suggest that it is likely that NO is released from the ferrous,  $\{\text{FeNO}\}_7$  state.<sup>2,13,59</sup> The fast release of NO from the  $\{\text{FeNO}\}_7$  intermediate may be attributed to a weak Fe–NO bonding in the ferrous nitrosyl adduct formed. The higher N–O stretching frequencies in the  $\{\text{FeNO}\}_n$  ( $n = 6, 7$ , and  $8$ ) species of FeTESP and FeDEsC suggested weak Fe–NO bonding, *i.e.*, four electron-withdrawing ester groups or two ester groups with two saturated carbon centers had an almost similar effect. Thus, heme  $d_1$ , which had two EW-keto groups and two saturated pyrrolic carbons, was likely to have a weaker Fe–NO bond relative to heme  $c$ , which has neither. A weaker Fe–NO in FeDEsC is associated with a large  $K_d$  for  $\text{NO}_2^-$  replacement relative to FeTPP consistent with the strong linear correlation between  $\nu_{\text{N-O}}$  and  $K_d$  observed for both enzymatic and synthetic systems. Similarly, a weaker Fe–NO in the heme  $d_1$  active site of  $\text{Cd}_1\text{NiR}$ , evident from a higher  $\nu_{\text{N-O}}$ , should result in higher NO (product)  $K_d$ , relative to  $\text{NO}_2^-$  (substrate). It might be envisaged that due to the ruffled nature of the isobacteriochlorin ring in heme  $d_1$ , they form weak  $\{\text{FeNO}\}_7$  species. But calculations of the ruffling parameters<sup>69</sup> suggested that maximum ruffling was present in  $\{\text{FeTPC-NO}\}_7$  species, which possess a chlorin ring (see the ESI, Section 9†), and had a relatively strong Fe–NO bond.

The  $\Delta G^\circ$  for PCET to the  $\{\text{FeHNO}\}_8$ , the competing reaction to NO release, was affected by both  $E^\circ$  and  $\text{p}K_a$  of the  $\{\text{FeNO}\}_7$  species. Between FeDEsC–NO and FeTPC–NO, where the latter was devoid of EWGs, the  $\text{p}K_a$  of  $\{\text{FeNO}\}_8$  species increased by 1.92 units (Table 2), but it lowered the  $E^\circ$  of the  $\{\text{FeNO}\}_7/8$  redox process by  $\sim 90$  mV (Table 2), making the PCET to the  $\{\text{FeNO}\}_7$  species of FeTPC–NO slightly favorable, relative to FeDEsC–NO. By omitting both saturation and EWGs (FeTPP–NO), the  $E^\circ$  decreased while the  $\text{p}K_a$  of  $\{\text{FeNO}\}_8$  species increased which resulted in higher  $\text{BDFE}_{\text{NH}}$  of the  $\{\text{FeHNO}\}_8$  species but it was not as high as that of FeDEsP–NO. In the case of FeTESP–NO, where the saturation was absent but two more EWGs were present (relative to FeDEsC–NO), the  $E^\circ$  increased by  $\sim 280$  mV but the  $\text{p}K_a$  of  $\{\text{FeNO}\}_8$  species becomes too low to be protonated, resulting in  $\text{BDFE}_{\text{NH}}$  being lower than that of FeTPP–NO. Therefore, for a facile PCET, there needs to be a balance between  $E^\circ$  and  $\text{p}K_a$ , which was attained here in FeDEsP–NO. This model was equally applicable to the FeOEP system, where

the high  $\text{BDFE}_{\text{NH}}$  was due to the greater  $\text{p}K_a$  of the  $\{\text{FeNO}\}_8$  species. Introducing EW-keto groups increased the  $E^\circ$  but at the expense of the  $\text{p}K_a$  of  $\{\text{FeNO}\}_8$  species (Table 2), resulting in a gradual decrease in  $\text{BDFE}_{\text{NH}}$ . However, it should also be noted that  $\{\text{FeHNO}\}_8$  species is not very stable due to the disproportionation of the Fe–HNO unit. The  $\{\text{FeHNO}\}_8$  species could only be stabilized either with steric protection (bis-picket fence porphyrin<sup>46</sup> or globin chain in hemoglobin<sup>44,45</sup>) or in a highly electron-rich porphyrin like FeOEP ( $\nu_{\text{NO}/\{\text{FeNO}\}_7} = 1665$   $\text{cm}^{-1}$ ).<sup>41,70–72</sup> Hence, it is not surprising that  $\{\text{FeHNO}\}_8$  species in electron-deficient octabromo[tetrakis(pentafluorophenyl)]porphyrin, Fe(TFPBr<sub>8</sub>) (NO) ( $\nu_{\text{NO}/\{\text{FeNO}\}_7} = 1726$   $\text{cm}^{-1}$ )<sup>54</sup> could not be isolated. The weak  $\text{BDFE}_{\text{NH}}$  and weaker  $\{\text{FeNO}\}_7$  adduct likely bias the FeDEsC (which has two EWGs along with two saturated pyrrolic carbons, like heme  $d_1$  in the active site of  $\text{Cd}_1\text{NiR}$ ) for NO dissociation. In contrast, stronger  $\text{BDFE}_{\text{NH}}$  driven by a favourable balance between  $\text{p}K_a$  (due to better back-bonding to the NO  $\pi^*$ -orbitals) and  $E^\circ$  is responsible for facile PCET to  $\{\text{FeNO}\}_7$  to produce  $\{\text{FeHNO}\}_8$  which is necessary to eventually release  $\text{NH}_4^+$  in  $\text{CcNiR}$ .

## Conclusion

In summary, the results on structural variants of iron-porphyrins suggested that  $\text{Cd}_1\text{NiR}$  does not proceed with the PCET process to form  $\{\text{FeHNO}\}_8$  intermediate, due to its lower  $\text{BDFE}_{\text{NH}}$  arising from the weaker back-donation from heme  $d_1$  where the EWGs and  $\text{sp}^3$  peripheral carbons enhance competitive back-bonding from the iron to the porphyrinoid  $\pi^*$  and NO  $\pi^*$ -orbitals. The weaker back-bonding to the bound NO results in a weaker Fe–NO bond and hence, it releases NO. In  $\text{CcNiR}$ , on the other hand, heme  $c$  has greater back-bonding to the NO from iron, which strengthens the Fe–NO bond and tunes the  $\text{p}K_a$  allowing PCET to occur to form  $\{\text{FeHNO}\}_8$  species, which is crucial for the further reactions to release  $\text{NH}_4^+$ .

## Experimental details

### Materials

All reagents were of the highest grade commercially available. Iodine, trifluoroacetic acid (TFA), 2,3-dichloro-5,6-dicyano-1,4-









- 29 C. K. Chang and W. Wu, *J. Biol. Chem.*, 1986, **261**, 8593–8596.
- 30 A. M. Stolzenberg, S. H. Strauss and R. H. Holm, *J. Am. Chem. Soc.*, 1981, **103**, 4763–4778.
- 31 S. Ozawa, E. Sakamoto, Y. Watanabe and I. Morishima, *J. Chem. Soc., Chem. Commun.*, 1994, 935–936, DOI: 10.1039/C39940000935.
- 32 Y. Liu and M. D. Ryan, *Inorg. Chim. Acta*, 1994, **225**, 57–66.
- 33 Y. Liu, C. DeSilva and M. D. Ryan, *Inorg. Chim. Acta*, 1997, **258**, 247–255.
- 34 C. K. Chang, K. M. Barkigia, L. K. Hanson and J. Fajer, *J. Am. Chem. Soc.*, 1986, **108**, 1352–1354.
- 35 S. Ozawa, E. Sakamoto, T. Ichikawa, Y. Watanabe and I. Morishima, *Inorg. Chem.*, 1995, **34**, 6362–6370.
- 36 D. W. Feng, Y. S. Ting and M. D. Ryan, *Inorg. Chem.*, 1985, **24**, 612–617.
- 37 E. Fujita and J. Fajer, *J. Am. Chem. Soc.*, 1983, **105**, 6743–6745.
- 38 D. Lancon and K. M. Kadish, *J. Am. Chem. Soc.*, 1983, **105**, 5610–5617.
- 39 C. K. Chang and J. Fajer, *J. Am. Chem. Soc.*, 1980, **102**, 848–851.
- 40 M. H. Barley and T. J. Meyer, *J. Am. Chem. Soc.*, 1986, **108**, 5876–5885.
- 41 M. H. Rahman and M. D. Ryan, *Inorg. Chem.*, 2017, **56**, 3302–3309.
- 42 Y. Liu and M. D. Ryan, *J. Electroanal. Chem.*, 1994, **368**, 209–219.
- 43 I. K. Choi, Y. Liu, D. Feng, K. J. Paeng and M. D. Ryan, *Inorg. Chem.*, 1991, **30**, 1832–1839.
- 44 M. R. Kumar, D. Pervitsky, L. Chen, T. Poulos, S. Kundu, M. S. Hargrove, E. J. Rivera, A. Diaz, J. L. Colón and P. J. Farmer, *Biochemistry*, 2009, **48**, 5018–5025.
- 45 R. Lin and P. J. Farmer, *J. Am. Chem. Soc.*, 2000, **122**, 2393–2394.
- 46 L. E. Goodrich, S. Roy, E. E. Alp, J. Zhao, M. Y. Hu and N. Lehnert, *Inorg. Chem.*, 2013, **52**, 7766–7780.
- 47 C. K. Chang, *Biochemistry*, 1980, **19**, 1971–1976.
- 48 C.-B. Wang and C. K. Chang, *Synthesis*, 1979, **1979**, 548–549.
- 49 S. Amanullah, P. K. Das, S. Samanta and A. Dey, *Chem. Commun.*, 2015, **51**, 10010–10013.
- 50 J. K. Laha, S. Dhanalekshmi, M. Taniguchi, A. Ambroise and J. S. Lindsey, *Org. Process Res. Dev.*, 2003, **7**, 799–812.
- 51 L. W. Olson, D. Schaeper, D. Lancon and K. M. Kadish, *J. Am. Chem. Soc.*, 1982, **104**, 2042–2044.
- 52 L. A. Bottomley and K. M. Kadish, *Inorg. Chem.*, 1981, **20**, 1348–1357.
- 53 M. D. Bartberger, W. Liu, E. Ford, K. M. Miranda, C. Switzer, J. M. Fukuto, P. J. Farmer, D. A. Wink and K. N. Houk, *Proc. Natl. Acad. Sci. U.S.A.*, 2002, **99**, 10958.
- 54 J. Pellegrino, S. E. Bari, D. E. Bikiel and F. Doctorovich, *J. Am. Chem. Soc.*, 2010, **132**, 989–995.
- 55 L. E. Goodrich, F. Paulat, V. K. K. Praneeth and N. Lehnert, *Inorg. Chem.*, 2010, **49**, 6293–6316.
- 56 A. P. Hunt and N. Lehnert, *Acc. Chem. Res.*, 2015, **48**, 2117–2125.
- 57 K. M. Vogel, P. M. Kozlowski, M. Z. Zgierski and T. G. Spiro, *J. Am. Chem. Soc.*, 1999, **121**, 9915–9921.
- 58 C. M. Coyle, K. M. Vogel, T. S. Rush, P. M. Kozlowski, R. Williams, T. G. Spiro, Y. Dou, M. Ikeda-Saito, J. S. Olson and M. Z. Zgierski, *Biochemistry*, 2003, **42**, 10342.
- 59 S. Rinaldo, A. Arcovito, M. Brunori and F. Cutruzzola, *J. Biol. Chem.*, 2007, **282**, 14761–14767.
- 60 A. L. Speelman and N. Lehnert, *Acc. Chem. Res.*, 2014, **47**, 1106–1116.
- 61 Z. Wei and M. D. Ryan, *Inorg. Chem.*, 2010, **49**, 6948–6954.
- 62 A. E. Servid, A. L. McKay, C. A. Davis, E. M. Garton, A. Manole, P. S. Dobbin, M. A. Hough and C. R. Andrew, *Biochemistry*, 2015, **54**, 3320–3327.
- 63 J. J. Warren, T. A. Tronic and J. M. Mayer, *Chem. Rev.*, 2010, **110**, 6961–7001.
- 64 D. D. M. Wayner and V. D. Parker, *Acc. Chem. Res.*, 1993, **26**, 287–294.
- 65 V. Shafirovich and S. V. Lyman, *Proc. Natl. Acad. Sci. U.S.A.*, 2002, **99**, 7340.
- 66 M. A. Rhine, A. V. Rodrigues, R. J. B. Urbauer, J. L. Urbauer, T. L. Stemmler and T. C. Harrop, *J. Am. Chem. Soc.*, 2014, **136**, 12560–12563.
- 67 M. Ali, N. Stein, Y. Mao, S. Shahid, M. Schmidt, B. Bennett and A. A. Pacheco, *J. Am. Chem. Soc.*, 2019, **141**, 13358–13371.
- 68 M. C. Silvestrini, M. G. Tordi, G. Musci and M. Brunori, *J. Biol. Chem.*, 1990, **265**, 11783–11787.
- 69 T. Vangberg and A. Ghosh, *J. Am. Chem. Soc.*, 1999, **121**, 12154–12160.
- 70 W. R. Scheidt, H. F. Duval, T. J. Neal and M. K. Ellison, *J. Am. Chem. Soc.*, 2000, **122**, 4651–4659.
- 71 E. G. Abucayon, R. L. Khade, D. R. Powell, Y. Zhang and G. B. Richter-Addo, *J. Am. Chem. Soc.*, 2016, **138**, 104–107.
- 72 E. G. Abucayon, R. L. Khade, D. R. Powell, M. J. Shaw, Y. Zhang and G. B. Richter-Addo, *Dalton Trans.*, 2016, **45**, 18259–18266.
- 73 N. G. Connelly, P. T. Draggett, M. Green and T. A. Kuc, *J. Chem. Soc., Dalton Trans.*, 1977, 70–73, DOI: 10.1039/DT9770000070.
- 74 T. C. Harrop, Z. J. Tonzetich, E. Reisner and S. J. Lippard, *J. Am. Chem. Soc.*, 2008, **130**, 15602–15610.
- 75 M. J. Frisch, *Version C.02*, Gaussian, Inc., 2004.
- 76 R. Krishnan, J. S. Binkley, R. Seeger and J. A. Pople, *J. Chem. Phys.*, 1980, **72**, 650–654.
- 77 A. D. McLean and G. S. Chandler, *J. Chem. Phys.*, 1980, **72**, 5639–5648.
- 78 M. Cossi, N. Rega, G. Scalmani and V. Barone, *J. Comput. Chem.*, 2003, **24**, 669–681.
- 79 B. J. Littler, M. A. Miller, C.-H. Hung, R. W. Wagner, D. F. O'Shea, P. D. Boyle and J. S. Lindsey, *J. Org. Chem.*, 1999, **64**, 1391–1396.

